

# Effect of Bark Flour on Melt Rheological Behavior of High Density Polyethylene

Kamini Sewda, S. N. Maiti

Center for Polymer Science and Engineering, Indian Institute of Technology, New Delhi 110016, India

Received 27 May 2010; accepted 19 April 2011

DOI 10.1002/app.34715

Published online 23 August 2011 in Wiley Online Library (wileyonlinelibrary.com).

**ABSTRACT:** The melt rheological behavior of neem bark flour (BF) filled high density polyethylene (HDPE) has been studied at varying volume fraction ( $\Phi_f$ ) from 0 to 0.26 at 180, 190, and 200°C in the shear rate range from 100 to 5000  $s^{-1}$  using extruded pellets of the composites. The melt viscosity of HDPE increases with  $\Phi_f$  because the BF particles obstruct the flow of HDPE. With the incorporation of the coupling agent HDPE-g-MAH, the viscosity decreased compared to the corresponding compositions in the HDPE/BF systems due to a plasticizing/lubricating effect by HDPE-g-MAH. The composites obeyed power law behavior in the

melt flow. The power law index decreases with increase in the filler content and increases with temperature for the corresponding systems while the consistency index showed the opposite trend. The activation energy for viscous flow exhibited inappreciable change with either  $\Phi_f$  or inclusion of the coupling agent, however, the pre-exponential factor increased with filler concentration. © 2011 Wiley Periodicals, Inc. *J Appl Polym Sci* 123: 2122–2130, 2012

**Key words:** high density polyethylene; melt viscosity; power law; consistency index; activation energy

## INTRODUCTION

Since the late 1980s natural bio based fillers have attracted the attention of researchers due to their ecological and economical advantages. Various studies have been reported on the wood plastic composites (WPC) and their advantages.<sup>1–5</sup> There is a market growing exponentially all over the world due to which natural waste materials such as wood and bark flour, saw dust, rice husk, jute, and banana fibers have been used for value added end products.

Studies of rheological properties of polymeric materials are essential for evaluation of the polymer processing parameters like mold temperature, extrusion pressure in extrusion process, and injection molding conditions. The rheological behavior of polymer melt is mainly governed by the molecular weight, molecular weight distribution, and the degree of branching present in the structure of the polymer.<sup>6</sup> In particulate filled polymer systems, various factors related to fillers such as particle shape, size, structure, concentration, and dispersion in the polymer matrix affect the rheological properties. From these studies, interaction between the filler and the matrix may also be evaluated.

Various fillers are added to the polymer to obtain the required properties at a reasonable cost without much compromise to other properties. In general, with the addition of fillers the melt viscosity increases especially at higher filler concentrations which may lead to processing problems. In these composites, coupling agents are often used to modify the interphase between the filler and the matrix polymer. Although the coupling agents are used to enhance the interaction between the filler and the matrix very often they reduce the melt viscosity easing the flow and processing.<sup>6</sup>

High density polyethylene (HDPE) is a very useful commodity plastic with high chemical resistance, excellent electrical insulation, environmental resistance, and easy moldability. The interaction between the polymer and the filler plays an important role in maintaining the interparticle network and rheological properties of the filled polymer systems.<sup>7</sup> The higher the interaction between the matrix and the filler particles, the lesser the tendency of the filler particles to cluster and the better the dispersion. Wood flour and HDPE are chemically opposite in nature being polar and nonpolar, respectively. The interaction between HDPE and wood flour may be enhanced with the introduction of a suitable coupling agent, maleic anhydride grafted HDPE (HDPE-g-MAH).

In wood plastic composites, the effect of coupling agent, (HDPE-g-MAH) on the interfacial wettability and composites performance in improving the material properties were investigated by many scientists.<sup>8</sup>

Correspondence to: S. N. Maiti (maiti@polymers.iitd.ernet.in or maitisn49@yahoo.co.in).

Contract grant sponsors: Council of Scientific and Industrial Research (CSIR).

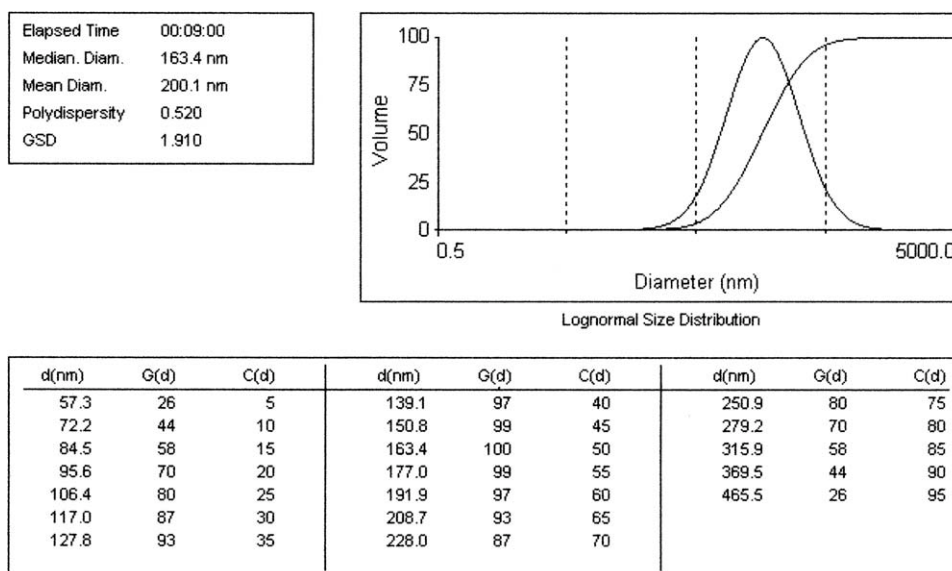


**Figure 1** Lognormal size distribution curve of BF particles having average particle diameter and median diameter was 163 and 200.1 nm respectively.

Son et al. studied the effect of maleic anhydride coupling agent on composites of paper sludge with HDPE, LDPE, and PP by varying the coupling agent content while Yang and coworkers studied the effect of concentration of MAH-*g*-PP on rice-husk flour reinforced PP composites.<sup>9,10</sup> Maiti and Hassan studied the melt rheological properties of polypropylene-wood flour composites and they found that the increase in melt viscosity and decrease in melt elasticity with increase in the concentration of wood flour.<sup>2</sup>

In this study, the melt rheological properties of HDPE/BF composites were evaluated and analyzed. The rheological parameters were evaluated such as melt viscosity and the activation energy for viscous flow at three temperatures, 180, 190, and 200°C, in the shear rate range 100–5000 s<sup>-1</sup>. The effect of incorporation of a coupling agent, HDPE-*g*-MAH, on the above properties have also been examined.

## EXPERIMENTAL

### Materials

Injection molding grade HDPE (G-Lex I58A180 density 0.95 g cm<sup>-3</sup>, MFI 18 g/10 min (230°C/2.16 kg load)) was obtained from the Gas Authority of India. (GAIL) and used as the matrix polymer.<sup>11</sup> Neem bark peeled off from a tree was cleaned with water, dried, and ground.<sup>12</sup> The resulting flour was first sieved through cotton cloth prior to the sieve analysis using mesh size 300–63 μm by mechanical vibratory sieve analyzer. BF particles lower than 63 μm mesh size was used as fillers for composite preparation. Further analysis for the particle size was per-

formed on a Brookhaven Instrument using 90 Plus particle Sizing Software Version 3.42, Figure 1. The average particle diameter and median diameter was 163 and 200.1 nm, respectively, (Figure 1), while the density was 1.36 g cm<sup>-3</sup> (measured by specific gravity bottle). Maleic anhydride grafted high density polyethylene (HDPE-*g*-MAH), (OPTIM TP-506/E, density 0.954 g cm<sup>-3</sup>, MFI = 1.24 g/10 min at 230°C and 2.16 kg load, maleic anhydride content (%) 0.99, acid number 11) from Pluss Polymers, India and used as a coupling agent.<sup>13</sup> The coupling agent content was 5 wt % based on the filler.

### Compounding: Twin screw extruder

Vacuum dried BF (60°C) and HDPE were dry blended followed by melt blending at varying volume fraction ( $\Phi_f$ ) of the BF from 0 to 0.26 (0–50 phr) in a corotating twin screw extruder, Model JSW J75E IV-P ( $L/D = 36$ ; diameter  $D = 30$  mm) at screw speed of 174 rpm. The temperature ranged from 140–180°C from the feed zone to die zone. The extruded strands were granulated. Neat HDPE was also passed through the same processing conditions to maintain identical thermal shear history.

### Measurements

#### Rheometry measurements

The melt rheological studies were performed on an advanced dual-bore (Bagley corrected) capillary rheometer from Bohlin Instruments, Rosand RH7, using a capillary die. The shear flow analysis was performed using a capillary die in one bore and an orifice die in the other. The capillary die was with  $L/D$

= 10 where  $L = 10$  mm and  $D = 1$  mm. The orifice die was of zero length ( $L = 0.25$  mm) with  $D = 1$  mm. The software "Flow Master" was used for the analysis of the data. In the steady shear experiment, the shear rate range used was from 100 to 5000  $\text{s}^{-1}$  at three temperatures 180, 190, and 200°C. All the data were both Bagley and Rabinowitch corrected.

The apparent shear rate,  $\dot{\gamma}_a$ , (Newtonian fluid) at the wall of the capillary is represented by eq. (1)<sup>6,14</sup>:

$$\dot{\gamma}_a = \left( \frac{4Q}{\pi R_c^3} \right) (\text{s}^{-1}), \quad (1)$$

where  $R_c$  is the capillary die radius (cm) and  $Q$  is the volumetric flow rate ( $\text{cm}^3 \text{s}^{-1}$ ) given by eq. (2):

$$Q = \frac{AS}{t} = Av (\text{cm}^3 \text{s}^{-1}), \quad (2)$$

where  $v$  is piston speed ( $\text{cm s}^{-1}$ ),  $A$  is area ( $\text{cm}^2$ ),  $S$  is piston path (cm), and  $t$  is time (s).

The true shear rate at the wall of capillary,  $\dot{\gamma}_w$ , was calculated using the  $\dot{\gamma}_a$  values by applying the Rabinowitsch-Weissenberg correction, eq. (3)<sup>15,16</sup>:

$$\dot{\gamma}_w = \left( \frac{3n+1}{4n} \right) \left( \frac{4Q}{\pi R_c^3} \right) (\text{s}^{-1}), \quad (3)$$

$$\dot{\gamma}_w = \left( \frac{3n+1}{4n} \right) \dot{\gamma}_a (\text{s}^{-1}), \quad (4)$$

where  $n$  is the flow behavior index obtained from the slope of log of apparent shear rate ( $\log \dot{\gamma}_a$ ) versus log shear stress ( $\log \tau_w$ ) plot. The log-log plot of shear stress and shear rate gives the slope  $n$  which is also known as Power-Law exponent. The value of  $n = 1$  stands for Newtonian behavior,  $n < 1$  denotes pseudoplastic behavior (thermoplastics) and indicated the shear thinning behavior while  $n > 1$  is for shear-thickening behavior.

The apparent melt shear viscosity,  $\eta_a$ , is given by the relations in eqs. (5) and (6)<sup>15,16</sup>:

$$\eta_a = \frac{\text{Shear stress}}{\text{Shear rate}} = \frac{\tau_w}{\dot{\gamma}_w} (\text{Pa. s}), \quad (5)$$

$$\eta_a = K \dot{\gamma}_w^{n-1}. \quad (6)$$

The relation between  $\tau_w$  and  $\dot{\gamma}_w$  is given by the "power law (Ostwald-de waele)" eq. (7):

$$\tau_w = K \dot{\gamma}_w^n, \quad (7)$$

where  $K$  is the consistency index. Generally  $K = 10^3$  to  $10^5$  Pa.s and  $n = 0.8$  to  $0.2$ . Viscosity of polymeric materials generally decreases with increase in the shear rate. The reduction in the viscosity is due to the molecular alignment of polymer chains along the

flow direction and disentanglement of polymer chains.

#### Influence of temperature on melt viscosity

The exponential dependence of melt viscosity on temperature is given by the semi-logarithmic Arrhenius equation.<sup>17-19</sup>

$$\eta_a = A \exp\left(\frac{\Delta E}{RT}\right). \quad (8)$$

Here,  $A$  is a constant, characteristic of the polymer,  $T$  the absolute temperature,  $\Delta E$  the activation energy for viscous flow, and  $R$  the universal gas constant. The activation energy for the viscous flow is calculated from the slope of the  $\log \eta_a$  versus  $1/T$ .

## RESULTS AND DISCUSSION

### Steady shear stress–shear rate curves

Figure 2 shows the variations of shear stress ( $\log \tau_w$ ) against shear rate ( $\log \dot{\gamma}_w$ ) at three temperatures, 180, 190, and 200°C, for the HDPE/BF composites which were calculated from the volumetric flow measurement by fixing the temperature and varying the pressure. It can be observed that the curves follow linear increase in the shear stress with increase in the shear rate. Also the flow curves show gradual increase upwards with the increase in the filler concentration. This suggests that the shear stress–shear rate relationship follows the power law, eq. (6). It is clear that at a fixed shear rate the shear stress values of the composites were higher than those of the neat HDPE and the parameter goes on increasing with increase in the filler concentration. It means that the BF increases the shear stress, the increase is a function of the  $\Phi_f$ . Similar observations were reported in other filled systems also.<sup>20-22</sup> At higher shear rates the flow curves of the composites tend to converge with each other. This may imply that variation in the BF content has lower effect on the flow curves at higher shear rates compared to the lower shear rate values.

At high shear rates, the filler-polymer phase interaction force is overcome enabling the polymer flow carrying along the BF particles. The filler particles may also facilitate decrease in polymer chain entanglement thus easing the flow.

At lower temperature, the difference between the flow curves was more and all the curves were well separated whereas the separation decreases with increase in temperature as well as shear rate. This behavior may indicate that at higher shear rates and higher temperatures the convergence of the curve is due to the effect of decreased chain entanglement

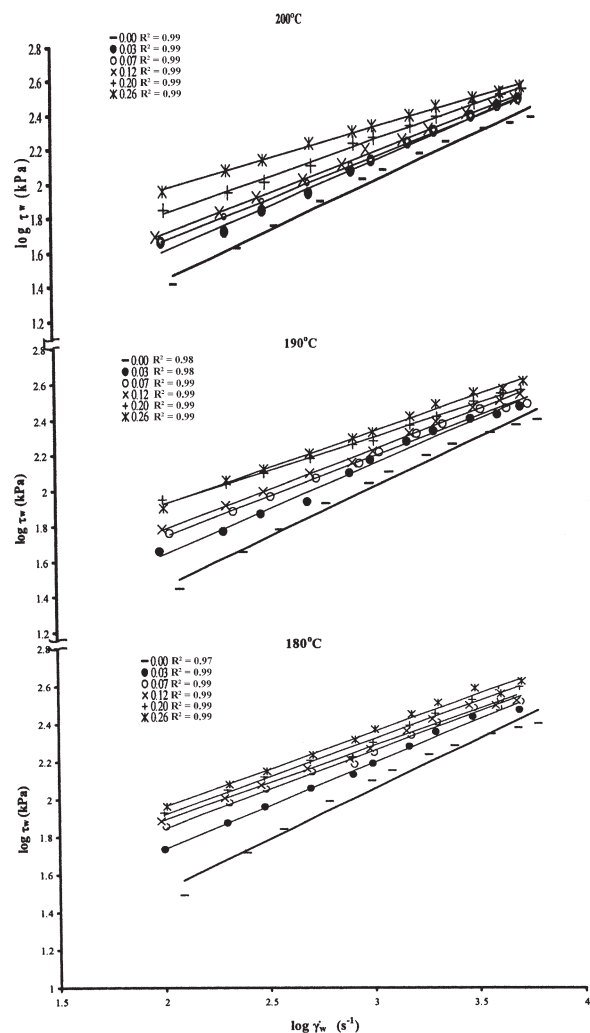


**Figure 2** Variations of  $\log \tau_w$  against  $\log \dot{\gamma}_w$  at three temperatures, 180, 190, and 200°C, for the HDPE/BF composites.

greater orientation of the polymer chains brought about by the BF particles.<sup>23</sup> Also, the separation between the curves was prominent at lower shear rates. This kind of behavior may be attributed to the relative predominance of extensional flow over shear flow in presence of the BF particles. Extensional flow dominates at low shear rates, usually below  $1000 \text{ s}^{-1}$  while shear flow is prominent at high shear rates.<sup>24,25</sup> The presence of BF particle introduces heterogeneity and discontinuity in HDPE, thus the flow was hindered.

Rheological behavior of the HDPE/BF/HDPE-g-MAH composites were also investigated and Figure 3 presents the shear stress versus shear rate plots. The response trends of the flow curves were similar to those of the HDPE/BF systems; the actual data were different, however. The convergences of the curves were more prominent at 200°C, in particular at higher ranges of the shear rates. This may be due to the greater disentanglement and sequential greater

alignment of the polymer chains due to a plasticizing/lubricating effect by the coupling agent similar to other systems.<sup>3,26,27</sup> The flow curve at  $\Phi_f = 0.26$  intersect the flow curves at  $\Phi_f = 0.12$  and 0.2 which may be due to an extent of greater disentanglement of the polymer chains brought about by the higher concentration of the filler.

### Melt viscosity

The apparent melt viscosity ( $\eta_a$ ) versus shear rate ( $\dot{\gamma}_w$ ) plots for the HDPE/BF and the HDPE/BF/HDPE-g-MAH composite systems at three temperatures 180, 190, and 200°C are presented in Figures 4 and 5, respectively. The melt viscosity decreases with the increase in the shear rate for all the composites

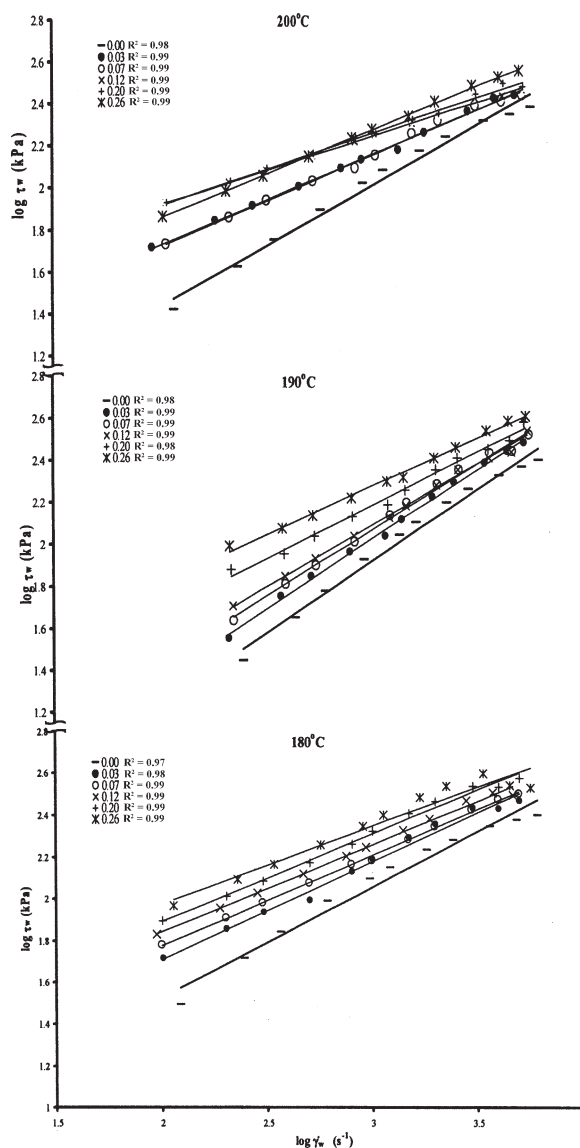


**Figure 3** Variations of  $\log \tau_w$  against  $\log \dot{\gamma}_w$  at 180, 190, and 200°C, for the HDPE/BF/HDPE-g-MAH composites.

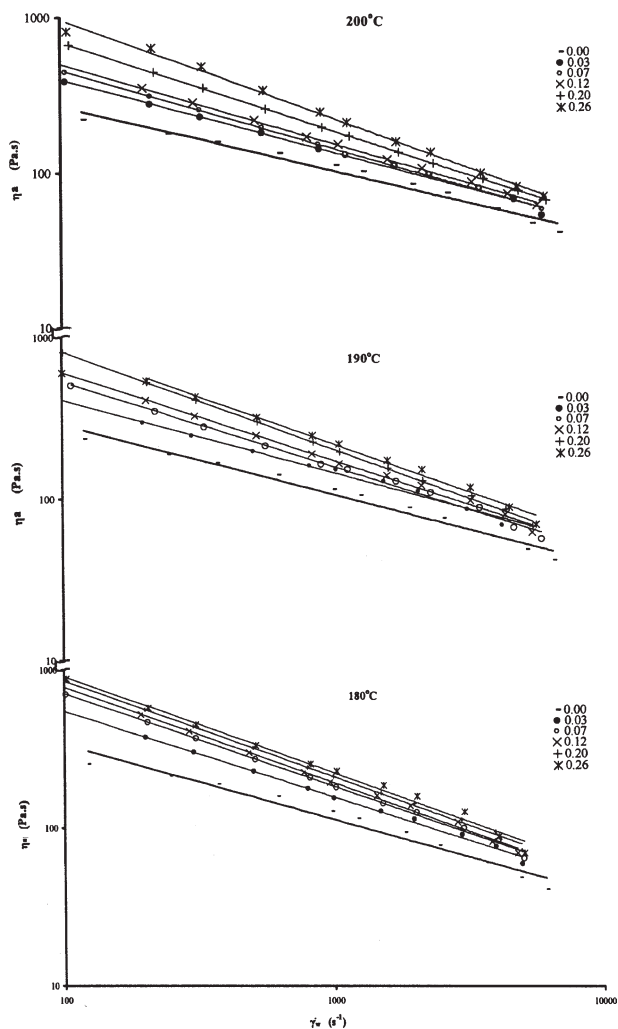


**Figure 4** Plots of  $\eta_a$  versus  $\dot{\gamma}_w$  for the HDPE/BF composites at three temperatures 180, 190, and 200°C.

irrespective of the filler or the presence of the coupling agent. The melt viscosity decrease is due to the disentanglement and alignment of the polymer molecules at high shearing forces. For the HDPE/BF composites the melt viscosity increases with the filler concentration. It can be seen in Figure 6 that at a fixed shear rate of  $3000 \text{ s}^{-1}$  the melt viscosity increases with  $\Phi_f$ . This may be attributed to the BF particles' hindering the flow of the polymer melt similar to other systems.<sup>25,26,28</sup> The melt viscosity of any system depends on the mobility of the polymer chains at molecular level and the force acting on them, and is affected by a very slight change of environment, for example, incorporation of any inclusion.<sup>29</sup> At molecular level, the flow occurs when the polymer chains slide past each other. When a filler is added to a polymer, the resistance to flow increases due to filler particles' hindrance to the sliding between intermolecular layers. The resistance to the intermolecular slide enhanced with  $\Phi_f$ .

In the HDPE/BF/HDPE-g-MAH composite systems, the melt viscosity shows lower values at corresponding shear rates and concentrations of the filler compared to those of the HDPE/BF systems. This may be attributed to the plasticizing/lubricating effect of the low molecular weight fractions of the coupling agent, that is, low molecular weight HDPE chains formed due to the degradation of some of the grafted HDPE which facilitate the flow of HDPE. The plasticizing effect was prominent than the chemical bonding and physical interaction. The wetting of surface of BF particles by the HDPE may lead to the reduction in the friction forces facilitating the flow of the HDPE. The reduction in the viscosity in presence of the coupling agent may be due to lowering of the surface energy at the interphase of the polymer and the filler as observed in other works also.<sup>30,31</sup>

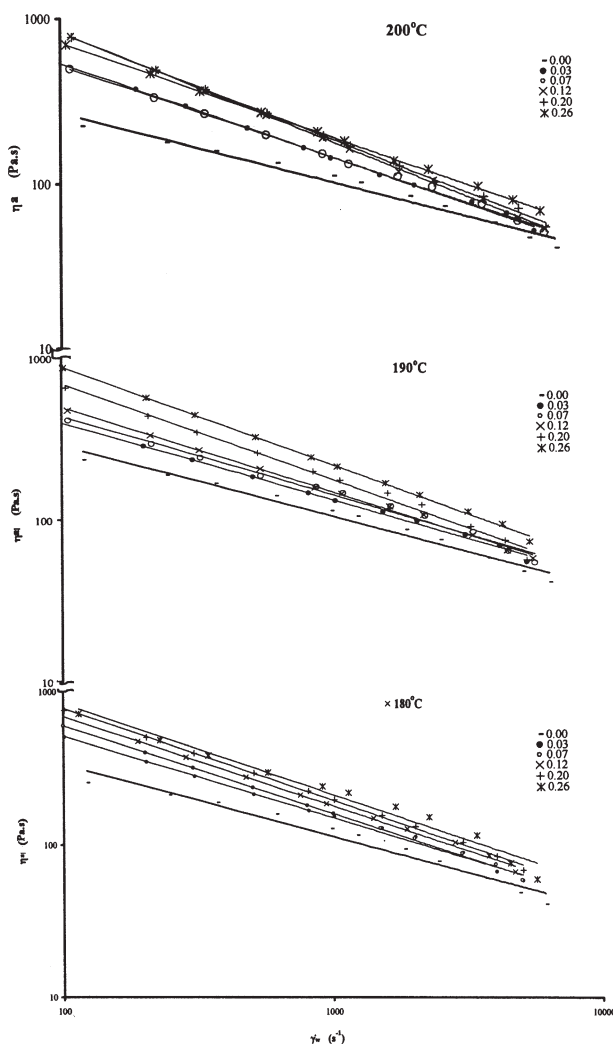


**Figure 5** Plots of  $\eta_a$  versus  $\dot{\gamma}_w$  for the HDPE/BF/HDPE-g-MAH composites at three temperatures 180, 190, and 200°C.

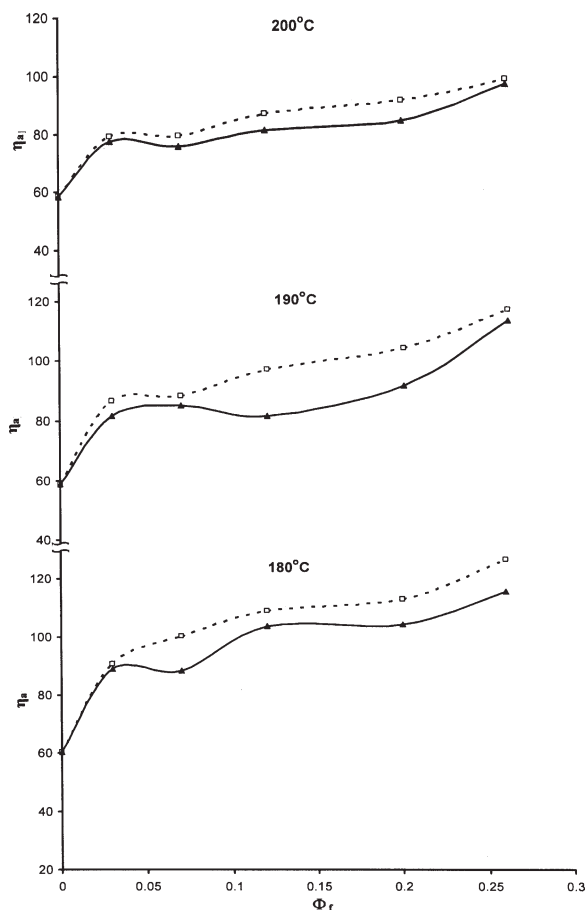


**Figure 6** Plots of  $\eta_a$  versus  $\Phi_f$  for the HDPE/BF ( $\square$ ) and the HDPE/BF/HDPE-g-MAH ( $\blacktriangle$ ) composites at three temperatures 180, 190, and 200°C.

The melt flow process depends on the molecular chain mobility, bonding between the two phases and the entanglements due to other molecules or filler particles. It appears that the chemical interaction between the coupling agent and the BF particles and the chain entanglement between HDPE moieties are overridden by the viscous forces at melt temperatures under shear.

In addition, the plasticizing/lubricating function by the low molecular HDPE (as stated earlier) will also enhance the polymer flow and the shear thinning behavior. The critical temperature for HDPE-g-MAH degradation appears to be  $\sim 200^\circ\text{C}$  since at the grafting points the secondary carbon atom is converted to a tertiary carbon atom which is more prone to oxidative degradation.

### Significance of power law exponent

The values of the power law exponent ( $n$ ) are calculated from the slopes of the  $\log \tau_w$  versus  $\log \dot{\gamma}_w$  plots following eq. (7), Figure 7 and Table I, for the HDPE/BF and the HDPE/BF/HDPE-g-MAH composites. The values of  $n$  were less than unity thus

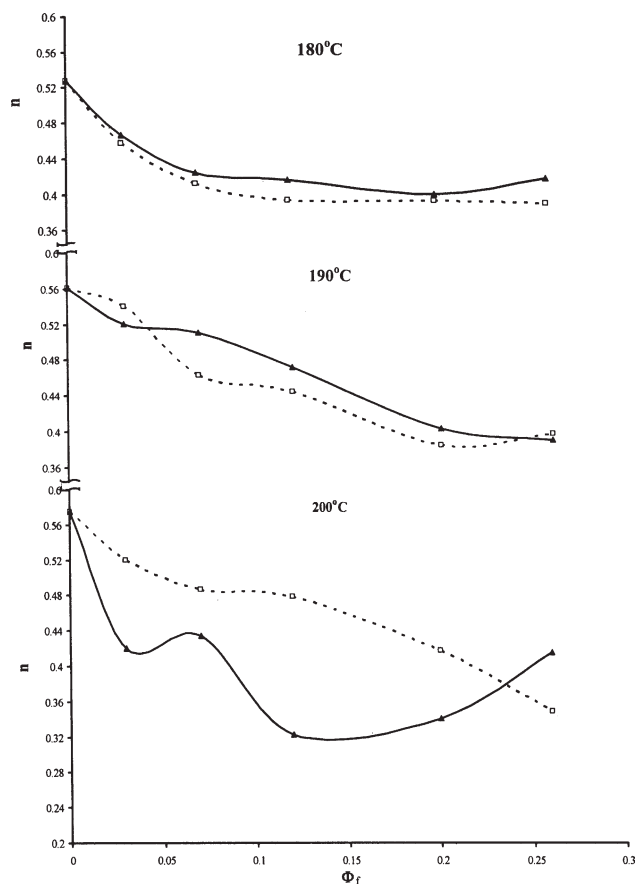


**Figure 7** Plots of  $n$  versus  $\Phi_f$  for the HDPE/BF ( $\square$ ) and the HDPE/BF/HDPE-g-MAH ( $\blacktriangle$ ) composites at three temperatures 180, 190, and 200°C.

indicating that the composites show pseudoplastic behavior at all the composite compositions. At all the temperatures the values of  $n$  decrease with increase in  $\Phi_f$  indicating that the BF particles enhance the shear thinning characteristics of HDPE. This may be due to the hindrance of HDPE chain entanglement in presence of the BF particles so that the molecules are easily oriented in the flow direction.<sup>3,26</sup> With increase in the temperature from 180 to 200°C, the values of  $n$  increase for the

**TABLE I**  
Values of the Power Law Coefficient ( $n$ ) at 180, 190, and 200°C Temperatures at Varying  $\Phi_f$

$\Phi_f$	Values of $n$					
	HDPE/BF			HDPE/BF/HDPE-g-MAH		
	180°C	190°C	200°C	180°C	190°C	200°C
0.00	0.5281	0.561	0.574	0.528	0.561	0.574
0.03	0.4573	0.541	0.52	0.466	0.52	0.42
0.07	0.412	0.462	0.486	0.425	0.51	0.434
0.12	0.3928	0.444	0.478	0.416	0.472	0.322
0.20	0.3924	0.384	0.417	0.4	0.403	0.34
0.26	0.3887	0.397	0.349	0.417	0.39	0.415

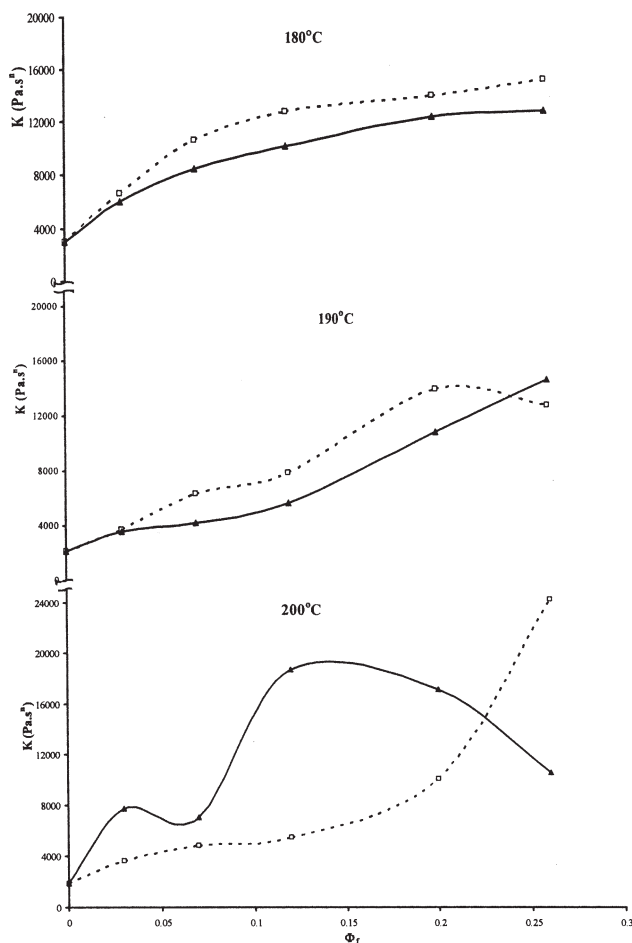


**Figure 8** Plots of  $K$  versus  $\Phi_f$  for the HDPE/BF ( $\square$ ) and the HDPE/BF/HDPE-g-MAH ( $\blacktriangle$ ) composites at 180, 190, and 200°C.

corresponding  $\Phi_f$  values. This is attributed to the fact that at lower temperature the filler obstructs the flow of HDPE, while the resistance to flow decreases at higher temperature, since the polymer molecules are more mobile. The polymer flow tends more towards Newtonian behavior to an extent.

In the HDPE/BF/HDPE-g-MAH composite systems, the variations of  $n$  versus  $\Phi_f$  at 180 and 190°C were quite similar to those of the HDPE/BF compo-

**TABLE II**  
Values of the Consistency Coefficient,  $K$  ( $\text{Pa s}^n$ ) at 180, 190, and 200°C Temperatures at Varying  $\Phi_f$

$\Phi_f$	Values of $K$					
	HDPE/BF			HDPE/BF/HDPE-g-MAH		
	180°C	190°C	200°C	180°C	190°C	200°C
0.00	2954.9	2168.9	1897.9	2954.9	2168.9	1897.9
0.03	6665.7	3729.3	3621.2	6011.1	3619.2	7745.2
0.07	10664	6361.6	4828	8528.5	4174.7	7028.4
0.12	12807	7884.8	5492.5	10183	5668.8	18694
0.20	13999	13937	10086	12383	10801	17139
0.26	15222	12763	24217	12818	14601	10578

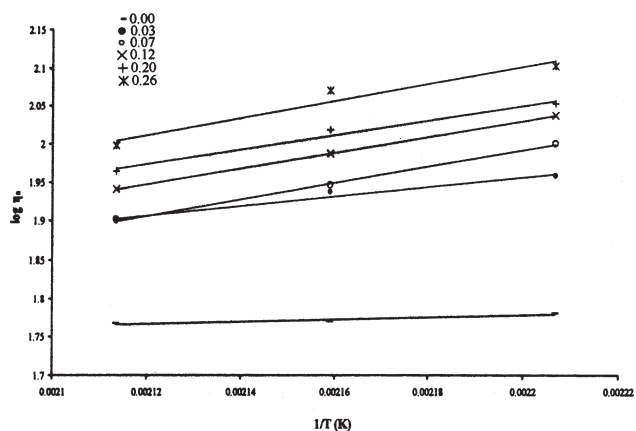


**Figure 9** Plots of  $\eta_a$  versus  $1/T$  for the HDPE/BF composites.

sites, the values were marginally higher than those for the HDPE/BF composites. This may be due to a degree of phase adhesion which hinders the shear thinning ability marginally. At 200°C, the values of  $n$  are, however, lower for the HDPE/BF/HDPE-g-MAH systems which may be due to the dominance of polymer flow at this high temperature which overcomes the effect of the coupling agent. In addition, the plasticizing/lubricating function by the low molecular weight decomposition product of HDPE-g-MAH, as stated earlier, will also enhance the polymer flow and shear thinning behavior.<sup>32,33</sup>

### Significance of consistency index

The values of the consistency index ( $K$ ) were determined from the intercept of the  $\log \tau_w$  versus  $\log \dot{\gamma}_w$  plots following the eq. (7), Figure 8 and Table II for the HDPE/BF and the HDPE/BF/HDPE-g-MAH composites. The variations of  $K$  with the filler concentration and temperature (180, 190, and 200°C) are plotted in Figure 8.

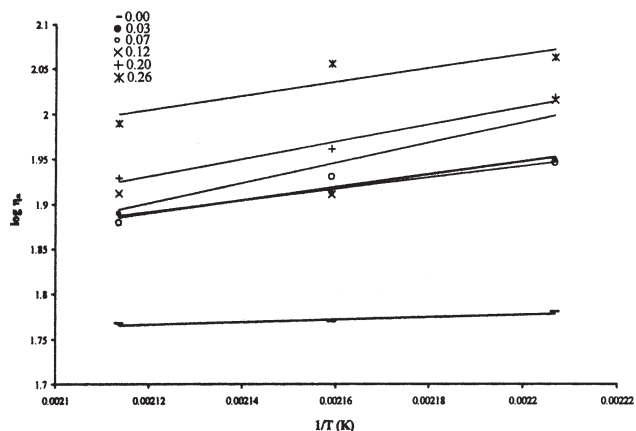


**Figure 10** Plots of  $\eta_a$  versus  $1/T$  for the HDPE/BF/HDPE-g-MAH composites.

**TABLE III**  
**Values of the Activation Energy for Viscous Flow ( $\Delta E$ )**  
**for the HDPE/BF and HDPE/BF/HDPE-g-MAH**  
**Composites at Shear Rate 3000 s<sup>-1</sup>**

$\Phi_f$	HDPE/BF	HDPE/BF/HDPE-g-MAH
	$\Delta E$ (kJ mol <sup>-1</sup> )	$\Delta E$ (kJ mol <sup>-1</sup> )
0.00	1.42	1.42
0.03	0.63	0.65
0.07	1.07	0.72
0.12	1.04	1.13
0.20	0.96	0.97
0.26	1.13	0.79

The consistency indices versus  $\Phi_f$  curves of the HDPE/BF composites at 180 and 190°C enhanced with  $\Phi_f$  which may be due to the enhancement of stiffness of the melt in presence of BF which increased with  $\Phi_f$ . At 200°C the  $K$  value also enhanced with  $\Phi_f$ , the value at  $\Phi_f = 0.26$  showed a significant increase. This may be attributed to the creation of an extent of turbulence at this temperature due to which the particles come into contact of the capillary wall enhancing the flow consistency.

In presence of the coupling agent, the data at 180 and 190°C also enhanced with  $\Phi_f$ , the values were, however, a degree lower than those of HDPE/BF systems. This may be due to the plasticizing/lubricating function by the coupling agent, as stated earlier. The  $K$  value at 200°C showed much increase in presence of the coupling agent up to  $\Phi_f = 0.2$ , whereas, at  $\Phi_f = 0.26$  the value drops to an extent. This may be attributed to the degradation of the grafted HDPE to low molecular weight fractions which facilitate the turbulence at 200°C enabling the BF particles coming into contact with the capillary wall in the process creating resistance to flow. The latter effect predominate the plasticizing/lubricating action of the coupling agent.

### Influence of temperature

The viscosity of the polymer melts decreases with increase in temperature because at higher temperatures the molecular motions are facilitated due to the availability of excess free volume. The melt viscosity of polymer was more sensitive to temperature as compared to the polymer composites or filled systems because only the polymer part of the composites contributes to the change in the free volume. The effect of temperature on the melt viscosity is obtained from the semi-logarithmic Arrhenius expression and the plot  $\log \eta_a$  versus  $1/T$  for all the composites, [eq. (8)].  $\Delta E$  values were evaluated from the slopes of these curves for HDPE/BF and HDPE/BF/HDPE-g-MAH composites, Figures 9 and 10 respectively, Table III. It may be observed that the

activation energy for viscous flow show insignificant variation with  $\Phi_f$  in both the systems. However, filler addition leads to increase in the pre-exponential factor  $A$  which may be attributed to the increase in the efficient size of viscous flow kinetic units in presence of the filler. Similar observations were reported in other systems also.<sup>2,20,34</sup>

### CONCLUSION

The HDPE/BF and HDPE/BF/HDPE-g-MAH composites exhibit power law behavior in the melt flow. The shear stress increases with shear rate and BF concentration. Melt viscosity also increases with BF content in the HDPE/BF composites while the increase in the parameter in the HDPE/BF/HDPE-g-MAH systems were marginally lower due to plasticizing/lubricating function of the coupling agent.

The power law index decreases in the HDPE/BF composites with increase in  $\Phi_f$ , while with increase in temperature the value of  $n$  increases except at  $\Phi_f = 0.26$  at 200°C where an extent of turbulence decreases the  $n$  value. In the HDPE/BF/HDPE-g-MAH composites the values of  $n$  also decreased with increase in  $\Phi_f$ , the data were marginally higher due, possibly, to the existence of phase interaction between at 180 and 190°C. At 200°C the  $n$ - $\Phi_f$  plot runs lower than that of the HDPE/BF systems due to enhanced disentanglement of the polymer chains brought about by low molecular weight decomposition product of the grafted coupling agent. With increase in temperature the  $n$  values enhance in both the systems.

The variations in the activation energy for viscous flow were insignificant in both the systems; however, the trend of the data variation were similar. The pre-exponential factor increased with  $\Phi_f$ , the dependence of the parameter on the filler concentration was also similar in presence of the coupling agent.

### References

- Li, T. Q.; Wolcott, M. P. *Polym Eng Sci* 2005, 45, 549.
- Maiti, S. N.; Hassan, M. R. *J Appl Polym Sci* 1989, 37, 2019.
- Maiti, S. N.; Subbarao, R.; Ibrahim, M. N. *J Appl Polym Sci* 2004, 91, 644.
- Maiti, S. N.; Singh, K. *J Appl Polym Sci* 1986, 32, 4285.
- Sewda, K.; Maiti, S. N. *J Appl Polym Sci* 2007, 105, 2598.
- Dealy, J. M.; Wissbrun, K. F. *Melt Rheology and its Role in Plastics Processing: Theory and Applications*; Kluwer Academic: USA, 1999.
- Bigg, D. M. *Polym Eng Sci* 1983, 23, 206.
- Li, Q.; Matuana, L. M. *J Thermoplast Compos Mater* 2003, 16, 551.
- Son, J.; Yang, H.-S.; Kim, H.-J. *J Thermoplast Compos Mater* 2004, 17, 509.
- Yang, H.-S.; Wolcott, M. P.; Kim, H.-S.; Kim, S.; Kim, H.-J. *Polym Test* 2006, 25, 668.
- Product Literature, GAIL. Available at <http://www.gailonline.com/petrochemicals/i58a180.htm>.



12. Pushpak, Natural Black Emery Stone, Kirmani Engineering Industry, 22 Godam, Jaipur, India.
13. Pluss Polymers, F-213/B, 1st Floor, Lado Sarai, New Delhi 110030, India. Available at [www.plusspolymers.com](http://www.plusspolymers.com).
14. Ferguson, J.; Kemblowski, Z. *Applied Fluid Rheology*; Elsevier Applied Science: Amsterdam, 1991.
15. Brydson, J. A. *Flow Properties of Polymer Melts*; Iliffe: London, 1978.
16. Middleman, S. *The Flow of High Polymers: Continuum and Molecular Rheology*; Wiley-Interscience: New York, 1968.
17. Mckelvy, J. M. *Polymer Processing*; Wiley: New York, 1962.
18. Gupta, R. K.; Nielsen, L. E. *Polymer and Composite Rheology*; Marcel Dekker: New York, 2000.
19. Shenoy, A. V. *Rheology of Filled Polymer Systems*; Dordrecht: Kluwer Academic Publishers, 1999.
20. Han, C. D. *J Appl Polym Sci* 1974, 18, 821.
21. Joshi, M.; Maiti, S. N.; Misra, A. *Polymer* 1994, 35, 3679.
22. Han, C. D.; Van Den Weghe, T.; Shete, P.; Haw, J. R. *Polym Eng Sci* 1981, 21, 196.
23. Utracki, L. A.; Catani, A. M. *Polym Eng Sci* 1985, 25, 690.
24. Gupta, A. K.; Kumar, P. K.; Ratnam, B. K. *J Appl Polym Sci* 1991, 42, 2595.
25. Martuscelli, E.; Silvestre, C.; Abote, G. *Polymer* 1982, 42, 229.
26. Li, T. Q.; Wolcott, M. P. *Compos A* 2004, 35, 303.
27. Maiti, S. N.; Singh, G.; Ibrahim, M. N. *J Appl Polym Sci* 2003, 87, 1511.
28. Basu, D.; Banerjee, A. N.; Misra, A. *J Appl Polym Sci* 1992, 46, 1999.
29. Couch, M. A.; Binding, D. M. *Polymer* 2000, 41, 6323.
30. Arroyo, M.; Perez, F.; Vigo, J. P. *J Appl Polym Sci* 1986, 32, 5105.
31. Saini, D. R.; Shenoy, A. V.; Nadkarni, V. M. *Polym Eng Sci* 1985, 25, 807.
32. Wood-Plastic Composites.TechLine, F. P. L., Issued 01/04. <http://www.fpl.fs.fed.us/documnts/techline/wood-plastic-composites.pdf>.
33. Clemons, C. M.; Ibach, R. E. *Forest Products J* 2004, 54, 50.
34. Saini, D. R.; Shenoy, A. V.; Nadkarni, V. M. *Polym Compos* 1986, 7, 193.